Modelling Water Flow through a Multi-layered Cover Liner for a Waste Dump

C. J. Matthews[a], R.D. Braddock[a] and G.C. Sander[b]

[a] *Griffith University, Brisbane, Qld 4001, Australia (c.matthews@gu.edu.au)*
[b] *Loughborough University, Leicestershire, UK*

Abstract: When a waste dump or landfill reaches its full capacity, a cover liner is employed as a last measure to isolate the potentially harmful waste from the environment. One of the main functions of a cover liner is to prevent water from entering the waste thereby preventing any additional risk of groundwater pollution. Cover liners are usually constructed from various soil layers and therefore it is important to understand the behaviour of infiltrating water through such soil structures. In the past, numerical models have dealt predominantly with vertical infiltration and infiltration into sloping hillsides which are infinite in extent, in an attempt to understand flow phenomena through cover liners. The numerical model presented in this paper will deal with water flow through a more realistically shaped cover liner to expand our understanding of flow through sloping layered soils and multi-layered cover liner systems.

Keywords: Multi-layer; Soils; Landfill; Modelling

1. INTRODUCTION

When a waste disposal site reaches its full capacity, whether it be mining or municipal, a cover liner is employed as a last measure to isolate potentially harmful waste from the environment. Essentially, a cover liner is a multi-layered structure engineered from various soils and geo-synthetic materials that covers the waste. One of the main functions of a cover liner is to prevent infiltrating water from penetrating the underlying waste thereby minimising the risk of groundwater pollution. According to Koerner and Daniel [1997], the infiltration barrier is considered the most important aspect of a cover liner system. In the past, infiltration barriers have been predominantly made from compacted soils and geosynthetic material due to their low hydraulic conductivity properties. However, this technology has been questioned particularly in relation to longevity and the development of weak zones during and after construction [Donald and McBean, 1994; Murray et al., 1995].

In recent times, an alternative infiltration barrier known as the capillary barrier has been studied by several researchers [Ross, 1990; Oldenburg, 1993; Walter et al., 2000]. A capillary barrier is a fine over coarse soil structure that impedes the flow of water by the strong capillary forces of the fine soil at the soil layer interface. Water will only enter the coarse soil once the weight of the accumulating water has exceeded the air entry value of the coarse soil. If a capillary barrier is inclined, the water that is held at the interface will flow laterally down the slope. This type of flow behaviour is known as capillary divergence and is desirable for any cover liner system. Steady state analytical and experimental studies [Ross, 1990; Warrick et al., 1997; and Walter et al., 2000] have been conducted in an attempt to understand the behaviour of capillary divergence and to quantify the downslope length of the divergence. Similarly, numerical models have also been used as a tool to understand flow dynamics through capillary barriers and other multi-layered systems [Oldenburg, 1993; Fayer et al., 1992]. The majority of these studies have dealt with infiltration into vertical soil profiles or sloping soil profiles of infinite extent. Since these conditions are not realistic for a cover liner, there is a need to test previously documented behaviour on a more realistic model.

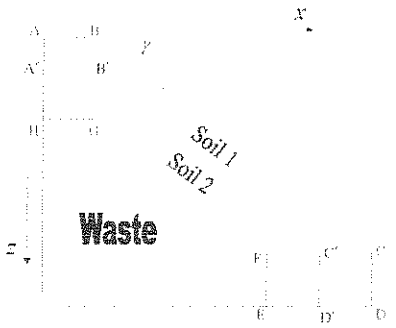

Figure 1. Piece-Wise Linear Cover Liner.

The cover liner model presented in this paper has a more realistic shape being piece-wise linear with a horizontal top, vertical bottom and a sloping section in-between (Figure 1). The lengths A-B and C-D, and A-H and D-E are related by $\tan(\gamma)$ where γ is the angle of the slope. This same relationship is also given to the step size in the x- and z-direction to ensure that nodal points within the grid system lie on the boundary. The cover liner consists of two soils overlaying a mound of waste with the soil layer interface mapped out by points A′-B′-C′-D′. The aim of this paper is to compare the transient behaviour of infiltrating water through the cover liner against documented behaviour. In particular, this study will concentrate on behaviour generated by Warrick's et al. [1997] steady state analytical solution.

2. COVER LINER MODEL

To model water flow through a multi-layered cover liner, the Method of Lines will be applied to the following head-based version of Richard's Equation:

$$C\frac{\partial h}{\partial t}=\frac{\partial}{\partial x}\left(K(h)\frac{\partial h}{\partial x}\right)+\frac{\partial}{\partial z}\left(K(h)\frac{\partial h}{\partial z}\right)-\frac{\partial K}{\partial z} \qquad (1)$$

where $C(=\partial\theta/\partial h)$ is the water capacity, θ is water content, h is hydraulic pressure, K is the hydraulic conductivity, z is the vertical axis positive downwards, x is the horizontal axis positive to the right and t is time. The initial condition at $t = 0$ is a constant hydraulic pressure (h_0) throughout the domain and the external boundary conditions are given by:

$$\text{A-B} \quad \frac{\partial h}{\partial z}=1-\frac{R_f}{K}, \qquad (2)$$

$$\text{B-C} \quad \frac{\partial h}{\partial z}-\tan(\gamma)\frac{\partial h}{\partial x}=1-\frac{R_f\cos(\gamma)}{K\cos(\gamma)}, \qquad (3)$$

$$\text{C-D, A-H, E-F} \quad \frac{\partial h}{\partial x}=0, \qquad (4)$$

$$\text{D-E} \quad \frac{\partial h}{\partial z}=0, \qquad (5)$$

$$\text{G-H} \quad \frac{\partial h}{\partial z}=1, \qquad (6)$$

$$\text{F-G} \quad \frac{\partial h}{\partial z}-\tan(\gamma)\frac{\partial h}{\partial x}=1, \qquad (7)$$

where R_f is a constant rainfall flux applied across the top of the cover liner. Along the bottom of the cover liner, a no flow condition is assumed with a no flow boundary on A-H and C-D as an axis of symmetry. Boundary D-E is given a natural drainage condition allowing water to flow from the cover liner.

On the internal boundary (A′-B′-C′-D′), two conditions must be satisfied at the interface, that is, the normal flux (q) and the hydraulic pressure (h) must remain continuous. The first condition is satisfied by using Darcy's Law to equate normal fluxes across the soil layer interface. This results in the following equations:

$$\text{A′-B′} \quad -K_1\left(\left.\frac{\partial h}{\partial z}\right|_1-1\right)=-K_2\left(\left.\frac{\partial h}{\partial z}\right|_2-1\right), \qquad (8)$$

$$\text{B′-C′} \quad -K_1\cos(\gamma)\left(\left.\frac{\partial h}{\partial z}\right|_1-1\right)+K_1\sin(\gamma)\left.\frac{\partial h}{\partial x}\right|_1 = -K_2\cos(\gamma)\left(\left.\frac{\partial h}{\partial z}\right|_2-1\right)+K_2\sin(\gamma)\left.\frac{\partial h}{\partial x}\right|_2, \qquad (9)$$

$$\text{C′-D′} \quad -K_1\left.\frac{\partial h}{\partial x}\right|_1=-K_2\left.\frac{\partial h}{\partial x}\right|_2, \qquad (10)$$

where the subscripts denote soil type as depicted in Figure 1. To satisfy the second condition, the above equations are usually solved iteratively for a given h on its corresponding boundary. However, as both boundaries merge into the corner point B′ or C′, Equations (8) and (9) and Equations (9) and (10) must be resolved on their respective corner points for a single nodal point within the system. This implies that there are four conditions to be satisfied by the two values of h_1 and h_2 at each of the points B′ and C′, and the system is overdetermined. Instead, a finite element grid formulation is used around each corner point that results in an expression for the transient behaviour at the corner points while conserving water around the corner point. This formulation results in a more physically realistic solution, which is easy to incorporate into the Method of Lines [Matthews et al., 2001].

To solve the system, the Method of Lines is used to reduce equation (1) to a set of ordinary differential equations (ODEs) by discretising the spatial part of the partial differential equation. To discretise equation (1), a finite differencing technique developed by Schiesser [1991] was used. The technique involves upwinding and downwinding finite differencing schemes to account for the boundaries of the domain. Unlike the traditional approach, boundary conditions are not explicitly incorporated into the scheme but are imposed, in the appropriate position, on either the h or the $\partial h/\partial z$ distribution vector. The choice of the distribution vector depends on the type of boundary condition [Schiesser, 1991]. The resultant set of ODE's from the Method of Lines is of the form:

$$\frac{\partial \mathbf{h}}{\partial t} = \mathbf{f}(\mathbf{h}, t), \qquad \mathbf{h}(z, x, 0) = \mathbf{h}_0, \tag{11}$$

where bold face represents a vector, $\mathbf{f}(\mathbf{h},t)$ is the resultant vector from applying the finite differencing scheme to the spatial derivatives in equation (1) and $\mathbf{h}_0$ is the initial h distribution vector. Equation (11) can be integrated by any conventional ODE integrator to advance the solution in time.

3. ANALYTICAL SOLUTION ON INFINITE SLOPES

As an extension to the work by Ross [1990] and Steenhuis et al. [1991], Warrick et al. [1997] developed a general solution for steady state flow of water through sloping layered soils of infinite extent. The solution allows any hydraulic functions for the K, C and θ-h relationships to be used and the solution holds for infinitely deep layers and finite multiply layered soils. For a finite upper layer and an infinite lower layer, the solution is as follows:

$$d\cos(\gamma) = \int_{h_2}^{h_1} \frac{dh}{\frac{q}{K_1(h)} - 1}, \tag{12}$$

$$Q_h = -\tan(\gamma) \int_{h_2}^{h_1} K_1(h)\, dh, \tag{13}$$

$$L = Q_h / q \tag{14}$$

where d is the depth of the upper layer, γ is the angle of the slope, h_1 is the hydraulic pressure at the top of the upper layer, h_2 is the hydraulic pressure at the soil layer interface, K_1 is the conductivity of the upper layer, Q_h is the total horizontal flow, L is the length of divergence of the flow and q is the predefined flux in and out of the system. Equation (12) provides a functional relationship between the depth of the upper layer and hydraulic pressure given the limiting hydraulic pressure (h_2) at the interface. The interface hydraulic pressure corresponds to the steady state solution of the lower infinite layer, which has a constant steady state hydraulic pressure profile.

From an analysis of Equation (12) to (14), Warrick et al. [1997] made four main observations about the behaviour of steady state flow through sloping layered soils. Firstly, from an analysis of equation (12), it was shown that the flow behaviour at the soil layer interface could be predominantly down-slope or up -slope depending on the conditions at the interface. This behaviour can be observed in either fine-over-coarse or coarse-over-fine soil structures and is determined by the following conditions:

$$\begin{aligned} q < K_1(h_2) &\Rightarrow Q_h > 0 \text{ (downward deflection)} \\ q > K_1(h_2) &\Rightarrow Q_h < 0 \text{ (upward deflection)} \end{aligned} \tag{15}$$

Essentially, upslope deflection occurs when the underlying layer is wetter than the upper layer at steady state. Conversely, the underlying layer must be drier than the upper layer for downslope deflection. Equation (13) highlights the relationship between slope and divergence, which is directly related by $\tan(\gamma)$, that is, the smaller the slope the smaller the deflection. Similarly, equation (14) highlights the inverse relationship between divergence length and the predefined flux.

To ascertain whether the above behaviour is evident in the cover liner model, six main simulations will be generated using a capillary barrier consisting of a clay loam over loam sand. The soils are described by the van-Genuchten hydraulic functions and the parameters are taken from Hills et al. [1989]. As an idea of contrast between the two soils, the saturated hydraulic conductivity for the clay loam is 0.131 m/day and loam sand is 5.41 m/day. To generate the six runs, the capillary barrier was simulated under varying angles and varying fluxes as summarised in Table 1. The magnitude of the fluxes are taken from Warrick et al. [1997].

Table 1: Estimate of horizontal flow and divergence length at varying angles and fluxes

	γ (degrees)	h_1 (m)	h_2 (m)	($m^2 year^{-1}$)	L (m)
$q = 0.1$ m $year^{-1}$					
Case 1:	15	-2.069	-1.956	0.0082	0.082
Case 2:	30	-2.069	-1.956	0.0178	0.178
$q = 1$ m $year^{-1}$					
Case 3:	15	-1.198	-1.227	-0.0064	-0.0064
Case 4:	30	-1.198	-1.227	-0.0138	-0.0138
$q = 10$ m $year^{-1}$					
Case 5:	15	-0.4163	-0.7501	-0.3025	-0.0303
Case 6:	30	-0.4163	-0.7501	-0.6518	-0.0652

For each simulation, the dump was given relatively small dimensions being 1 metre high with lengths AH = 0.3m and length A A′ = 0.18m. The length AB varied with the angle to keep the same number of nodes along it's length resulting in AB= 0.3m and AB=0.6m for 30 and 15 degrees respectively. Using equations (12) to (14) for a finite upper layer of 0.18m, approximations of horizontal flow and divergence length were evaluated for all six test cases, which are present in Table 1. For all test cases, the divergence lengths are small and, therefore, we would expect the development of a breakthrough region along the sloping interface and the flow behaviour predicted by equations (12) to (14). To determine this, all test cases where simulated for a period of 4.8 hours with an initial condition of $h = -1$ m through out the domain. At 4.8 hours, steady state is not reached but a convergence of flow behaviour does occur for some cases. The initial condition corresponds to a wet upper layer at approximately 80% of saturation and a dry lower layer, which is 20% saturated. Since the aim of the paper is to compare the behaviour in the transient state with observed behaviour of Warrick et al. (1997), which are for an infinite length slope, the following results will concentrate on the soil layer interface along the sloping region of the cover liner model.

4. RESULTS

Figure 2 shows a plot of the scaled normal flux against the length of the slope for Cases 1 and 3 at $t = 4.8$ hours. The normal flux is scaled by the saturated hydraulic conductivity of soil 1, as an estimate of the flux moving across the sloping interface relative to the hydraulic properties of the upper layer. In Figure 2, the scaled normal flux is given as a function of position along the sloping interface, where the down-slope distance is measured from B′ as zero (see Figure 1).

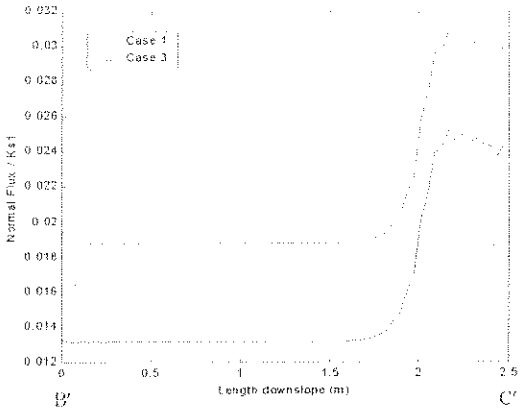

Figure 2. Scaled Normal Flux vs downslope length for $\gamma = 15$ degrees.

The difference between Case 1 and Case 3 is due to the magnitude of the flux into the system, with Case 1 being ten times less than Case 3 (Table 1). Therefore, it is evident from Figure 2 that the higher the flux, the higher the leakage rate across the sloping interface and this agrees with the behaviour described by Warrick et al. [1997]. In addition, it is apparent from Figure 2 that more water is infiltrating through the interface at the bottom of the slope close to C′ with a slight decrease as C′ is approached. This behaviour is to be expected since the area downslope will be significantly wetter than the upslope region creating a greater chance of breakthrough. The slight down-turn in the graph at C′ is likely to be the influence of the corner point region creating a greater lateral flow. The graph also shows slight oscillations near both corner points, which could be numerical error from the finite element grid. At lower angles, the grid is significantly deformed in the x-direction decreasing the ability of the finite element grid to accurately conserve water.

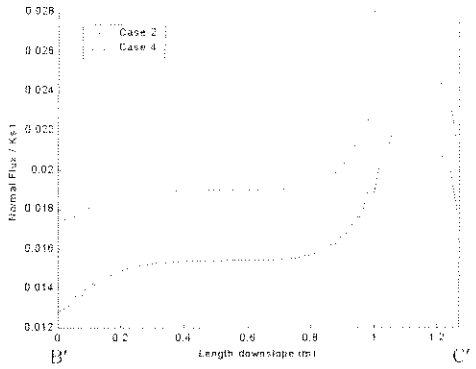

Figure 3. Scaled Normal Flux vs downslope length for $\gamma = 30$ degrees.

Figure 3 shows the graph of scaled normal flux against downslope length for Cases 2 and 4 at t = 4.8 hours. For these cases, the steeper angle has resulted in a shorter downslope length since the height of the dump is kept constant at 1 metre. Again, the same trends are observed with increase in flow across the interface for higher fluxes as well as towards the bottom of the slope. Comparing Figures 2 and 3, shows the effect of the change in angle with less water crossing the interface for the steep cover liner. Also, there is higher down-turn in the magnitude of normal flux as the slope approaches C′ suggesting there is a much larger lateral flow around the bottom corner point for steeper angles. In addition, slight oscillations are still present in Figure 3 and are roughly the same order of magnitude.

Unfortunately, Cases 5 and 6 could not be represented in the form shown in Figures 2 and 3, because the magnitude of the normal flux dwarfed the behaviour of the other two cases. A similar problem occurs when plotting the normal flux behaviour for Cases 5 and Case 6 on the same graph. The normal flux behaviour of Case 5 is shown in Figure 4; the same trends are apparent in Case 6 but are not shown.

As to be expected, there is a higher leakage rate across the whole sloping surface for Case 6 as compared to Figure 2 and 3. However, the most notable difference is the large leakage rates at the corner point B′ and C′. The flow behaviour at B′ is probably due to equivalent leakage rates at the top horizontal boundary (A′-B′), which subsequently affects the sloping region. For the bottom corner point, the reason is not as obvious but is probably due to a combination of high leakage at the bottom of the slope and leakage across the vertical interface boundary. In addition, numerical error may also be adding to the effect at C′, which can be an order of magnitude higher than at B′ [Matthews et al., 2001].

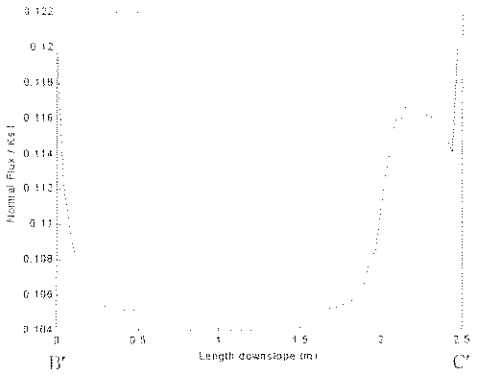

Figure 4. Scaled Normal Flux vs downslope length for $\gamma = 15$ degrees.

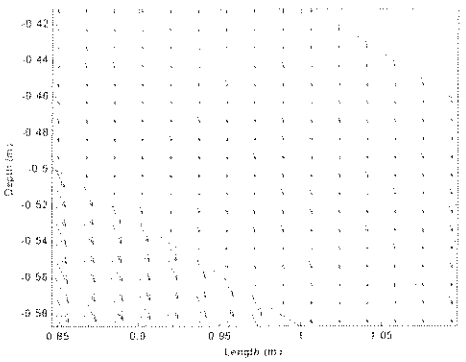

Figure 5. Downslope divergence for Case 2 at t = 1 day.

To determine whether a downslope and upslope divergence exists within the model, quiver plots, using flux components normal to the slope and parallel to the slope, were generate for Cases 2 and 6 and are presented in Figures 5 and 6, respectively. The figures show a magnification of the cover liner at approximately the middle of the slope around the soil layer interface. From Figure 5, it is obvious that downslope divergence exists which visually appears to be much greater than the steady state prediction of 17cm in Table 1. This is to be expected since the lower layer will become wetter as the system approaches steady state thereby decreasing the divergence length. In addition, this case needed a relatively long simulation period before the divergence behaviour became visually prominent which was due to the top soil having a fairly wet initial condition. Under these conditions, infiltration is initially driven by capillary forces for a fine soil causing infiltration to be predominantly normal to the slope.

Nevertheless, earlier simulation times did show positive fluxes parallel to the slope confirming the existence of downslope divergence.

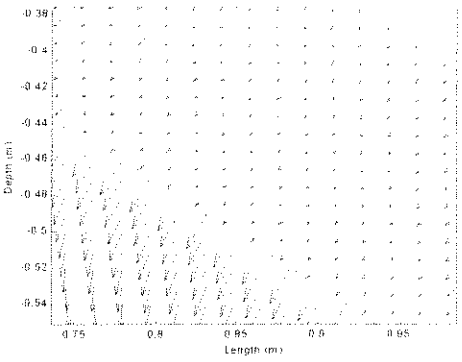

Figure 6. Downslope divergence for Case 6 at t = 4.8 hours.

Unlike Case 2, Case 6 showed upslope divergences at an earlier simulation period of 4.8 hours. This is probable due to the high leakage rates across the interface particular at the top of the cover liner. The upslope divergence is only slight in comparison to Figure 5 but appears to be greater than the predicted 6.5cm from the solution of Warrick et al. [1997]. As time advanced, the upslope divergence decreased and appeared to be normal to the slope at t = 1 day. However, the flux component parallel to the slope remained negative for all simulation periods confirming the upslope flow behaviour.

5. CONCLUSION

From the results, the cover liner model displayed the four main flow behaviours described by the analytical steady state solution of Warrick et al. [1997]. Given that an increase in leakage rates corresponds to a decrease in length of divergence, Figures 2, 3 and 4 confirm the direct relationship between divergence and angle (Equation (13)) and the inverse relationship between divergence and flux (Equation (14)). Figures 5 and 6, also confirm that the model simulates upslope divergence as well as downslope divergence for the appropriate cases suggested by Warrick et al. [1997]. The role of the corner points (B′ and C′) in terms of divergence is unclear but has the potential to increase lateral flow and minimising leakage. Therefore, for future research, it would be desirable to obtain a solution at steady state for the cover liner model to see how it compares with Warrick's et al. [1997] analytical solution and study the effects of the corner points.

6. REFERENCES

Donald, S.B., and E.A., McBean, Statistical analyses of compacted clay landfill liners. Part 1: Model Development, *Canadian Journal of Civil Engineering*., 21, 872-882, 1994.

Fayer, M.J., M.L., Rockford, and M.D., Campbell, Hydrologic Modelling of Protective Barriers: Comparison of Field Data and Simulation Results, *Soil Science Society of America Journal*., 56, 690-700, 1992.

Hills, R.G., I., Porro, D.B., Hudson, and P.J., Wierenga, Modeling One-Dimensional Infiltration into Very Dry Soils. Part 1: Model Development and Evaluation, *Water Resource Research*., 25(6), 1259-1269, 1989.

Koerner, R.M., and D.E., Daniel, *Final Covers for Solid Waste Landfills and Abandoned Dumps*, ASCE Press, Virginia, 1997.

Matthews, C.J., R.D., Braddock, and G.C., Sander, Using a Finite Element Grid on Corner Points in Flow Models, (submitted for publication), 2001

Murray, G.B., E.A., McBean, and J.F., Sykes, Estimation of Leakage Rates through Flexible Membrane Liners, *Ground Water Monitoring and Remediation*., 15(4), 148-154, 1995.

Oldenburg, C.M., On Numerical Modeling of Capillary Barriers, *Water Resource Research*., 29(4), 1045-1056, 1993.

Ross, B., The Diversion Capacity of Capillary Barriers, *Water Resource Research*., 26(10), 2625-2629, 1990.

Schiesser, W., *The Numerical Method of Lines: Integration of Partial Differential Equations*, Academic Press Inc, San Diego, 1991.

Steenhuis, T.S., J.-Y., Parlange, and K.-J.S., Kung, Comment on: the diversion capacity of capillary barriers, *Water Resource Research*., 27(8), 2155-2156, 1991.

Walter, M.T., J.-S., Kim, T.S., Steenhius, J.-Y., Parlange, A., Heilig, R.D., Braddock J.S., Selker, and J., Boll, Funneled Flow Mechanisms in a Sloping Layered Soil: Laboratory Investigation, *Water Resource Research*., 36(4), 841-849, 2000.

Warrick, A.W., P.J., Wierenga, and L., Pan, Downward water flow through sloping layers in the vadose zone: analytical solutions for diversions, *Journal of Hydrology*, 192, 321-337, 1997.